Article:

Ruderman, M.S., Petrukhin, N.S. and Kataeva, L.Y. (2025) Non-linear damped standing slow waves in cooling coronal magnetic loops. Monthly Notices of the Royal Astronomical Society, 542 (2). pp. 1076-1087. ISSN: 0035-8711

https://doi.org/10.1093/mnras/staf1310

Monthly Notices of the ROYAL ASTRONOMICAL SOCIETY

MNRAS **542,** 1076–1087 (2025) https://doi.org/10.1093/mnras/staf1310
Advance Access publication 2025 August 11

Non-linear damped standing slow waves in cooling coronal magnetic loops

M. S. Ruderman,[1,2,3]★ N. S. Petrukhin[4] and L. Y. Kataeva[5]

[1]*School of Mathematics and Statistics (SoMaS), The University of Sheffield, Hicks Building, Hounsfield Road, Sheffield S3 7RH, UK*
[2]*Space Research Institute (IKI) Russian Academy of Sciences, Moscow 117997, Russia*
[3]*Moscow Center for Fundamental and Applied Mathematics, Lomonosov Moscow State University, Moscow 119991, Russia*
[4]*National Research University Higher School of Economics, Moscow 101000, Russia*
[5]*Nizhny Novgorod State Technical University n.a. Alekseev, Department of Digital Economy, Minin St. 24, Nizhny Novgorod 603950, Russia*

Accepted 2025 August 7. Received 2025 August 7; in original form 2025 May 30

ABSTRACT

We study standing non-linear sausage waves in coronal loops with the plasma temperature varying with time. In our analysis we use the simplest model of a coronal loop in the form of a straight magnetic tube with a circular cross-section. We also assume that the plasma-beta is low. This enables us to neglect the magnetic field variation and consider standing waves occurring in a tube with rigid boundaries. Then the plasma motion is described by pure gas-dynamic equations. The background plasma temperature can vary with time, however we assume that its density remains constant. We consider perturbations with small amplitudes and use the Reductive Perturbation Method to derive the governing equations for standing waves. We show that a standing non-linear wave is a superposition of two identical non-linear waves propagating in the opposite directions in a complete analogy with the linear theory. Each of the two propagating non-linear waves are described by a modified Burgers equation that reduces to the standard Burgers equation when the plasma temperature does not change. The modified Burgers equation contains only one dimensionless parameter R determining the relative strength of non-linearity and dissipation related to viscosity and thermal conduction. It also contains one arbitrary function related to the background plasma temperature variation. We then assume that the temperature either increases or decreases exponentially. We study the standing waves in three cases: When dissipation strongly dominates non-linearity, when non-linearity strongly dominates dissipation, and when they are of the same order. The main conclusion that we make on basis of our analysis is that plasma cooling weakens the wave damping.

Key words: MHD – plasmas – waves – Sun: corona – Sun: oscillations.

1 INTRODUCTION

The Solar Ultraviolet Measurements of Emitted Radiation (SUMER) spectrometer on board of *SOHO* spacecraft observed standing waves in hot ($T \gtrsim 6$ MK) coronal loops (Kliem et al. 2002; Wang et al. 2002, 2003a, b). The oscillation periods of the observed waves ranged from 11 to 31 min, and the decay time from 5.5 to 29 min. These waves were interpreted by Ofman & Wang (2002) as slow standing waves. The velocity amplitude in these waves was up to one quarter of the phase speed implying that non-linearity can play an important role in their evolution. Ofman & Wang (2002) modelled the slow standing waves numerically. They found that the main damping mechanism is thermal conduction. For reviews of standing slow waves in coronal loops see Wang (2011) and Wang et al. (2021).

Ofman & Wang (2002) used the direct numerical solution of the 1D non-stationary non-linear equations for compressible fluids with the account of viscosity and thermal conduction. They considered only a restricted range of parameters. Later a similar modelling has been performed by Mendoza-Briceño, Erdélyi & Sigalotti (2004), Sigalotti, Mendoza-Briceño & Luna-Cardozo (2007), and Verwichte et al. (2008) for a wider range of coronal loop parameters and the initial perturbation amplitude.

It is often observed that oscillating coronal loops are cooling with the characteristic time on the order of a few oscillation periods (e.g. Aschwanden & Terradas 2008). Morton & Erdélyi (2008, 2010) and Ruderman (2011a, b) studied the effect of cooling on kink oscillations of coronal loops. Later Al-Ghafri et al. (2014) and Al-Ghafri (2015) extended this study to slow waves. These authors used the linear approximation.

Recently Ruderman, Petrukhin & Kataeva (2025) (Paper I below) studied non-linear propagating slow waves in cooling coronal loops. Ruderman (2013) (Paper II below) analytically studied non-linear standing slow waves in magnetic flux tubes. He assumed that all equilibrium quantities are constant. We aim to extend the analysis in Paper I and Paper II and study non-linear standing slow waves in cooling magnetic flux tubes. The paper is organized as follows: In the next section we describe the equilibrium state and present the governing equations. In Section 3 we derive the equations governing the evolution of non-linear standing waves. In Section 4 we consider the case where dissipation strongly dominates non-linearity and the waves are described by linear equations. In Section 5 we study the opposite case where non-linearity strongly dominates dissipation and the latter can be neglected. In Section 6 we investigate the generic

★ E-mail: M.S.Ruderman@sheffield.ac.uk

case and study the competition between non-linearity and dissipation. Section 7 contains the summary of the results and our conclusions.

2 EQUILIBRIUM STATE AND GOVERNING EQUATIONS

We study slow standing waves in hot coronal loops with the temperature $T \gtrsim 6$ MK. In these hot loops the atmospheric scale height exceeds 300 Mm. Hence, we can safely neglect the density variation along a loop if the height of the loop apex point is smaller than or of the order of 100 Mm. The plasma number density in hot loops is usually not higher than 10^{15} m^{-3}. Then, for $T \leq 10$ MK, the plasma pressure does not exceed 0.23 Nm^{-2}. Then we easily find that the plasma beta is smaller than 0.6 when $B \gtrsim 10^{-3}$ Tesla = 10 G. Although this value of plasma beta is not small it is still less than unity. If $B = 20$ G then we obtain plasma beta equal to 0.15, which is much smaller than unity. In accordance with these estimates we use the low-beta plasma approximation and neglect the magnetic field perturbation when studying the slow waves in hot coronal loops. This approximation greatly simplifies the analysis because this enables us to neglect the variation of the loop cross-section and the equilibrium quantities in the directions perpendicular to the loop axis. Neglecting in addition the loop curvature we can describe the slow waves by 1D hydrodynamic equations (Priest 1982; Goedbloed & Poedts 2004)

$$\frac{\partial \rho}{\partial t} + \frac{\partial (\rho u)}{\partial x} = 0, \tag{1}$$

$$\frac{\partial u}{\partial t} + u\frac{\partial u}{\partial x} = -\frac{1}{\rho}\frac{\partial p}{\partial x} + \frac{1}{\rho}\frac{\partial}{\partial x}\rho\nu\frac{\partial u}{\partial x}, \tag{2}$$

$$\frac{\partial T}{\partial t} + u\frac{\partial T}{\partial x} + (\gamma - 1)T\frac{\partial u}{\partial x} = \frac{\partial}{\partial x}\kappa\frac{\partial T}{\partial x} + Q(\rho, T), \tag{3}$$

$$p = \frac{k_B}{m}\rho T. \tag{4}$$

Here u is the velocity, ρ density, p pressure, T temperature, γ the ratio of specific heats, k_B the Boltzmann constant, m the mean mass for particle ($m \approx 0.6 m_p$ in the solar corona, where m_p is the proton mass), and $Q(\rho, T)$ the generalized heat-loss function. The coefficients ν and κ are defined by

$$\nu = \frac{4\eta_0}{3\rho}, \quad \kappa = \frac{(\gamma - 1)mk_\parallel}{\rho k_B}, \tag{5}$$

where η_0 is the first viscosity coefficient in the Braginskii's expression for the viscosity tensor, and $k_\parallel$ is the thermal conductivity parallel to the magnetic field. These latter two quantities are given by (Braginskii 1965)

$$\eta_0 \approx n k_B T \tau_p, \tag{6}$$

and (Spitzer 1962; Priest 1982)

$$k_\parallel \approx 10^{-11} T^{5/2}\ \mathrm{W\,m^{-1}K^{-1}}, \tag{7}$$

where $n = \rho/m_p$ is the electron number density and τ_p is the proton collision time. It is given by the approximate expression

$$\tau_p \approx 1.66 \times 10^7 \frac{T^{3/2}}{n \ln \Lambda}\ \mathrm{s}, \tag{8}$$

where Λ is the Coulomb logarithm and the electron number density n is measured in m^{-3}. For typical conditions in hot loops $\ln \Lambda \approx 20$, and τ_p is approximately between 10 and 25 s.

The system of equations (1)–(4) is the same as was used in Papers I and II, and almost the same as was used by Ofman & Wang (2002). The only difference from the latter is that we neglected the term describing the viscous heating in the energy equation (3). The reason for this is the following. The term describing the viscous heating is quadratic with respect to perturbations (Priest 1982; Goedbloed & Poedts 2004). Below we derive the equation governing the evolution of non-linear perturbations using the expansion with respect to the characteristic dimensionless amplitude ϵ. When doing so we assume that dissipation is weak, so that only the linear dissipative terms contribute in the second-order perturbation with respect to ϵ. The contribution of non-linear dissipative terms only appear in the third-order approximation with respect to ϵ which is not used in our analysis.

We also do not include the term describing dissipation due to optically thin radiation. In the first studies of damping of standing slow waves in hot coronal loops this effect was not taking into account (Ofman & Wang 2002; De Moortel & Hood 2003). In the following studies the effect of optically thin radiation was included (De Moortel & Hood 2004; Pandey & Dwivedi 2006). Pandey & Dwivedi (2006) presented especially detailed investigation of the efficiency of various damping mechanisms. In particular, they showed that the relative importance of optically thin radiation for the wave damping increases with the increase of the plasma density in the loop. It also increases with the increase of the loop length, but decreases with the increase of the plasma temperature.

In the first studies of the effect of plasma cooling on slow standing waves in hot coronal loops the effect of optically thin radiation was neglected (Al-Ghafri et al. 2014; Al-Ghafri 2015). Hence, the linear theory of slow wave damping in hot coronal loops with account of optically thin radiation is an outstanding problem. Only when such a study is carried out it would be possible to include this effect in the non-linear theory. This is why we do not included it in the present analysis.

The system of equations (1)–(4) has to be supplemented with the boundary conditions. We assume that the magnetic loop is frozen in the dense photosphere, so that

$$u = 0 \quad \text{at} \quad x = 0,\ L, \tag{9}$$

where L is the loop length. Similar to Al-Ghafri et al. (2014) and Paper I we assume that the unperturbed density is constant, while the unperturbed plasma pressure depends on time and it is proportional to the unperturbed temperature. Hence, the unperturbed quantities are related by

$$p_0(t) = \frac{k_B}{m}\rho_0 T_0(t). \tag{10}$$

We also assume that the unperturbed velocity is zero. The variation of the unperturbed temperature is described by

$$\frac{\mathrm{d}T_0}{\mathrm{d}t} = Q(\rho_0, T_0). \tag{11}$$

3 DERIVATION OF THE GOVERNING EQUATION FOR THE OSCILLATION VELOCITY

Following Papers I and II we assume that the dissipation is weak and introduce the scaled coefficients $\bar{\nu} = \epsilon^{-1}\nu$ and $\bar{\kappa} = \epsilon^{-1}\kappa$, where $\epsilon \ll 1$, and then use the Reductive Perturbation Method (Kakutani et al. 1968; Taniuti & Wei 1968). Here, it is quite imperative to emphasize that Pandey & Dwivedi (2006) separated all slow standing waves in hot coronal loops in strongly and weakly damped. The damping time of the former waves is of the order of the wave period, while the damping time of the latter waves is much greater than the wave period. This separation is perfectly accepted from the observational point of view. However, as it is explained in Paper II the characteristic time of oscillations is the oscillation period divided by 2π. Hence, from the theoretical point of view even oscillations with the damping time of the order of the wave period are weakly damped because the damping time is about six times greater than the characteristic time of oscillations. In accordance with this we introduce the scaled dissipation coefficients. By the way, it follows from this scaling that the effect of dissipation is only appeared in the second-order approximation. This implies that the propagation velocity of waves is the adiabatic sound speed. In the opposite limit of very large thermal conduction coefficient the propagation speed is isothermal sound speed. To describe this situation we need the scaling completely different from that used in our analysis. We assume that the characteristic time of variation of the plasma temperature and pressure is the characteristic time of oscillations times ϵ^{-1}. In accordance with this we introduce the 'slow' time $t_1 = \epsilon t$. Hence, p_0 and T_0 are the functions of t_1. We also assume that the oscillation amplitude is relatively small and neglect the effect of oscillations on ν and κ. Then it follows from equations (5)–(8) that

$$\nu = \nu_0 \left(\frac{T_0(t_1)}{T_{00}}\right)^{5/2}, \quad \eta = \eta_0 \left(\frac{T_0(t_1)}{T_{00}}\right)^{5/2}, \tag{12}$$

where ν_0, η_0, and T_{00} are the values of ν, η, and T_0 at $t = 0$. While the variation of the perturbation shape occurs on the slow time, there is also fast oscillations described by the 'normal' time t, so there are two times, normal and slow. To describe this two-time evolution of the system in geometrical optics all perturbations are taken in the form $w(t_1)\exp(i\epsilon^{-1}\Theta(t_1))$, where $\Theta(t_1) = (\pi/L)\int_0^{t_1} c(t')\,\mathrm{d}t'$ is eikonal. By analogy with the geometrical optics we introduce

$$X = \epsilon^{-1}\int_0^{t_1} c(t')\,\mathrm{d}t', \quad c^2(t) = \frac{\gamma p_0(t)}{\rho_0}, \tag{13}$$

where $c(t)$ is the unperturbed sound speed. Using the new variables we transform equations (1)–(4) to

$$c\frac{\partial \rho}{\partial X} + \frac{\partial(\rho u)}{\partial x} = -\epsilon\frac{\partial \rho}{\partial t_1}, \tag{14}$$

$$c\frac{\partial u}{\partial X} + u\frac{\partial u}{\partial x} + \frac{1}{\rho}\frac{\partial p}{\partial x} = -\epsilon\frac{\partial u}{\partial t_1} + \epsilon\bar{\nu}\frac{\partial^2 u}{\partial x^2}, \tag{15}$$

$$c\frac{\partial T}{\partial X} + u\frac{\partial T}{\partial x} + (\gamma - 1)T\frac{\partial u}{\partial x} = -\epsilon\frac{\partial T}{\partial t_1} + \epsilon\bar{\kappa}\frac{\partial^2 T}{\partial x^2}. \tag{16}$$

Equation (4) remains unchanged. When deriving equation (16) we took $Q(\rho, T) \approx Q(\rho_0, T_0)$, that is we neglected the variation of the generalised heat-loss function related to the density and temperature perturbation. If we take this variation into account then we arrive at the thermal misbalance problem in a cooling plasma. This problem was studied by many authors in a plasma with the constant unperturbed temperature (e.g. Kolotkov, Duckenfield & Nakariakov 2020; Kolotkov, Zavershinskii & Nakariakov 2021; Kolotkov & Nakariakov 2022; see also review by Nakariakov et al. 2024). We postpone studying the thermal misbalance problem in a cooling plasma till future research.

We look for the solution to the system of equations (4) and (14)–(16) with the boundary condition (9) in the form of expansions

$$f = f_0 + \epsilon f_1 + \epsilon^2 f_2 + \dots, \tag{17}$$

where f represents any of quantities u, ρ, p, and T. The first term, f_0, corresponds to the unperturbed state. We note that $u_0 = 0$, $\rho_0 =$ const, while p_0 and T_0 are functions of t_1.

3.1 First-order approximation

Substituting equation (17) in equations (4) and (14)–(16), and the boundary conditions equation (9), and collecting the terms of the order of ϵ yields

$$c\frac{\partial \rho_1}{\partial X} + \rho_0\frac{\partial u_1}{\partial x} = 0, \tag{18}$$

$$c\frac{\partial u_1}{\partial X} + \frac{1}{\rho_0}\frac{\partial p_1}{\partial x} = 0, \tag{19}$$

$$c\frac{\partial T_1}{\partial X} + (\gamma - 1)T_0\frac{\partial u_1}{\partial x} = 0, \tag{20}$$

$$p_1 = \frac{k_B}{m}(\rho_0 T_1 + T_0\rho_1). \tag{21}$$

The function u_1 must satisfy the boundary conditions

$$u_1 = 0 \quad \text{at} \quad x = 0,\ L. \tag{22}$$

Eliminating all variables in favour of u_1 from these equations and using the relation $c^2 = \gamma k_B T_0/m$ we obtain

$$\frac{\partial^2 u_1}{\partial X^2} - \frac{\partial^2 u_1}{\partial x^2} = 0. \tag{23}$$

The general solution to this equation can be written as

$$u_1 = c[f(\xi) + g(\eta)], \quad \xi = k(X - x), \quad \eta = k(X + x), \tag{24}$$

where k is an arbitrary constant with the dimension m^{-1}. We note that the functions f and g also depend on t_1, but at present we do not write this argument explicitly. Substituting equation (24) in equation (22) yields

$$f(kX) + g(kX) = 0, \quad f(kX - kL) + g(kX + kL) = 0. \tag{25}$$

It follows from these equations that $g(y) = -f(y)$ and $f(y)$ is a periodic function with the period $2kL$. It is convenient to have this period equal to 2π. Hence, we take $k = \pi/L$. Using equations (18)–(21) and (24) we obtain

$$u_1 = c[f(\xi) - f(\eta)], \quad \rho_1 = \rho_0[f(\xi) + f(\eta)], \tag{26}$$

$$p_1 = \rho_0 c^2[f(\xi) + f(\eta)], \quad T_1 = (\gamma - 1)T_0[f(\xi) + f(\eta)]. \tag{27}$$

3.2 Second-order approximation

In the second-order approximation we collect the terms of the order of ϵ^2 in equations (4) and (14)–(16), and the boundary conditions equation (9). Then using equations (24), (10), and (14)–(17) we obtain

$$c\frac{\partial \rho_2}{\partial X} + \rho_0\frac{\partial u_2}{\partial x} = 2c\rho_0 k(f_- f_-' + f_+ f_+') - \rho_0\left(\frac{\partial f_-}{\partial t_1} + \frac{\partial f_+}{\partial t_1}\right), \tag{28}$$

$$c\frac{\partial u_2}{\partial X} + \frac{1}{\rho_0}\frac{\partial p_2}{\partial x} = 2kc^2(f_- f_+' - f_+ f_-') - \frac{\partial(cf_-)}{\partial t_1} + \frac{\partial(cf_+)}{\partial t_1} + c\bar{\nu}k^2(f_-'' - f_+''), \tag{29}$$

$$c\frac{\partial T_2}{\partial X} + (\gamma - 1)T_0\frac{\partial u_2}{\partial x} = (\gamma - 1)\Big(kcT_0[\gamma(f_- f_-' + f_+ f_+') - (2 - \gamma)(f_- f_+' + f_+ f_-')] - \frac{\partial(T_0 f_-)}{\partial t_1} - \frac{\partial(T_0 f_+)}{\partial t_1} + \bar{\kappa}k^2 T_0(f_-'' + f_+'')\Big), \tag{30}$$

$$p_2 - \frac{k_B}{m}(\rho_0 T_2 + T_0\rho_2) = p_0(\gamma - 1)(f_- + f_+)^2, \tag{31}$$

$$u_2 = 0 \quad \text{at} \quad x = 0,\ L. \tag{32}$$

Here $f_- = f(\xi, t_1)$, $f_+ = f(\eta, t_1)$, and the prime indicates the derivatives with respect to ξ and η, respectively. Eliminating ρ_2, p_2, and T_2 from equations (28)–(31) we obtain the equation for u_2:

$$\begin{aligned}\frac{\partial^2 u_2}{\partial X^2} - \frac{\partial^2 u_2}{\partial x^2} &= k^2 c\big[(\gamma+1)\big(f_-'^2 + f_- f_-'' \\ &- f_+'^2 - f_+ f_+''\big) + (3-\gamma)(f_- f_+'' - f_+ f_-'')\big] \\ &- 2k\left(\frac{\partial f_-'}{\partial t_1} - \frac{\partial f_+'}{\partial t_1}\right) - k\frac{3\gamma-2}{\gamma c}\frac{\mathrm{d}c}{\mathrm{d}t_1}(f_-' - f_+') \\ &+ k^3\left(\bar{\nu} + \frac{(\gamma-1)\bar{\kappa}}{\gamma}\right)(f_-''' - f_+''').\end{aligned} \tag{33}$$

Since u_2 satisfies the boundary conditions (32) we can expand it in the Fourier series

$$u_2 = \sum_{n=1}^{\infty} U_n(X, t_1)\sin(knx). \tag{34}$$

It follows from equation (34) that the left-hand side of equation (33) has the form of the Fourier series expansion with respect to $\sin(knx)$. It is shown in Appendix A that the right-hand side of equation (33) can be also expanded in the Fourier series similar to equation (34). The Fourier expansions of various terms on the right-hand side of equation (33) are calculated in Appendix A. The coefficients at $\sin(knx)$ on the left and right-hand side must be equal. Then using equations (A5), (A6), (A8), (A10), and (A14) we obtain

$$\begin{aligned}\frac{\partial^2 U_n}{\partial X^2} + k^2 n^2 U_n &= 2kne^{iknX}\Bigg[ikc(\gamma+1)\sum_{m=-\infty}^{\infty} m f_m f_{n-m} \\ &- 2\frac{\partial f_n}{\partial t_1} - \frac{3\gamma-2}{\gamma c}\frac{dc}{dt_1}f_n - k^2\left(\bar{\nu} + \frac{(\gamma-1)\bar{\kappa}}{\gamma}\right)n^2 f_n\Bigg] \\ &- \frac{ick^2 n}{4}(3-\gamma)\sum_{m=-\infty}^{\infty}(n+2m)f_m f_{n+m}e^{ikX(n+2m)} + \text{c. c.},\end{aligned} \tag{35}$$

where c. c. stays for complex conjugate. The general solution to this equation is the sum of a particular solution of the inhomogeneous equation and the complementary function. If the right-hand side of equation (35) contains terms proportional to e^{iknX} and e^{-iknX} then a particular solution would contain terms proportional Xe^{iknX} and Xe^{-iknX}. Hence, the general solution to equation (35) is bounded only if the coefficients at terms proportional to e^{iknX} and e^{-iknX} on the right-hand side of this equation are zeros. We obtain the term proportional to e^{iknX} in the second term on the right-hand side of equation (35) taking $m = 0$, and the term proportional to e^{-iknX} taking $m = -n$. It follows from the condition $f_n(t_1) = 0$ for $n = 0$ that the coefficients at both terms are zero. Hence the only term proportional to e^{iknX} is the first term on the right-hand side of equation (35), and the only term proportional to e^{-iknX} is its complex conjugate. Therefore the solution to equation (35) is bounded only if the expression in the square brackets is zero:

$$ikc(\gamma+1)\sum_{m=-\infty}^{\infty} m f_m f_{n-m} - 2\frac{\partial f_n}{\partial t_1} - \frac{3\gamma-2}{\gamma c}\frac{\mathrm{d}c}{\mathrm{d}t_1}f_n - k^2\left(\bar{\nu} + \frac{(\gamma-1)\bar{\kappa}}{\gamma}\right)n^2 f_n = 0. \tag{36}$$

This equation for f written in terms of Fourier coefficients corresponds to the equation

$$\frac{\partial f}{\partial t_1}\frac{kc}{2}(\gamma+1)f\frac{\partial f}{\partial y} - \frac{k^2}{2}\left(\bar{\nu} + \frac{(\gamma-1)\bar{\kappa}}{\gamma}\right)\frac{\partial^2 f}{\partial y^2} + \frac{3\gamma-2}{2\gamma c}\frac{\mathrm{d}c}{\mathrm{d}t_1}f = 0. \tag{37}$$

The quantity $t_0 = 1/kc_0$ can be considered as the characteristic time for the oscillations, where c_0 is the value of c at $t = 0$. We introduce the dimensionless time $\tau = t_1/t_0 = \epsilon t/t_0$. Then using equation (12) and the relation $T_0/T_{00} = c^2/c_0^2$ we transform equation (37) to

$$\frac{\partial F}{\partial \tau} - \frac{\gamma+1}{2}F\frac{\partial F}{\partial y} - \frac{C^5}{R}\frac{\partial^2 F}{\partial y^2} - \frac{2-\gamma}{2\gamma C}\frac{\mathrm{d}C}{\mathrm{d}\tau}F = 0, \tag{38}$$

where $C = c/c_0$, $F = Cf$, and R can be considered as the geometric mean of the Reynolds and Peclet numbers at the initial time. It is defined by

$$\frac{1}{R} = \frac{\pi}{2\epsilon c_0 L}\left(\nu_0 + \frac{(\gamma-1)\kappa_0}{\gamma}\right). \tag{39}$$

When the equilibrium does not depend on time we have $c = c_0$ and the last term on the right-hand side of equation (38) is zero. Although equation (38) is written in variables different from those used in Paper II, it is easy to show that it coincides with equation (38) in Paper II when $c = c_0$. The substitution $F = -U$ reduces equation (38) to equation (33) in Paper I. Taking $u \approx \epsilon u_1$, $\tilde{\rho} = \rho - \rho_0 \approx \epsilon\rho_1$, $\tilde{p} = p - p_0 \approx \epsilon p_1$, and $\widetilde{T} = T - T_0 \approx \epsilon T_1$ we obtain from equations (24)–(26)

$$\begin{aligned}u &= \epsilon c_0[F(\xi,\tau) - F(\eta,\tau)], \\ \tilde{\rho} &= \frac{\epsilon\rho_0}{C}[F(\xi,\tau) + F(\eta,\tau)], \\ \tilde{p} &= \frac{\epsilon\rho_0 c_0^2}{C}[F(\xi,\tau) + F(\eta,\tau)], \\ \widetilde{T} &= \frac{\epsilon(\gamma-1)T_0}{C}[F(\xi,\tau) + F(\eta,\tau)].\end{aligned} \tag{40}$$

To solve equation (38) we must impose the initial condition for function F. It is natural to impose the initial conditions not directly on F but on the original variables u, $\tilde{\rho}$, $\tilde{p}$, and $\widetilde{T}$. The system of equations (1)–(4) is of the third order with respect to time. Hence, we must define three variables, for example, u, $\tilde{\rho}$, and $\widetilde{T}$ at $t = 0$. However, when deriving equation (23) we neglected an arbitrary function of t_1 to obtain the expressions for ρ_1, p_1, and T_1 in terms of u_1. This is equivalent to imposing the relation $\widetilde{T} = (\gamma-1)(T_0/\rho_0)\tilde{\rho}$ at $t = 0$. Hence, we consider not solutions to the most general initial value problem for the system of equations (1)–(4), but only solutions to the initial problem with $\tilde{\rho}$ and $\widetilde{T}$ satisfying this relation at $t = 0$. In accordance with this it is enough to define u and $\tilde{\rho}$ at the initial time:

$$u = \varphi(x), \quad \tilde{\rho} = \psi(x) \quad \text{at} \quad t = 0, \tag{41}$$

where $\varphi(x)$ and $\psi(x)$ are the $2L$-periodic functions and $\varphi(0) = \varphi(L) = 0$. Using equation (40) and the expressions for ξ and η we obtain from this equation

$$\begin{aligned}cF(-kx, 0) - F(kx, 0) &= c_0^{-1}\varphi(x), \\ F(-kx, 0) + F(kx, 0) &= \rho_0^{-1}\psi(x).\end{aligned} \tag{42}$$

It follows from these equations that

$$F(kx, 0) = \frac{\psi(x)}{2\rho_0} - \frac{\varphi(x)}{2c_0} \equiv \Phi(kx), \tag{43}$$

where $\Phi(y)$ is a 2π-periodic function.

4 SOLUTION FOR $R \ll 1$

In this section we consider the case where $R \ll 1$. This implies that the effect of dissipation strongly dominates the effect of non-linearity and we can use the linear approximation. Then equation (38) reduces to

$$\frac{\partial F}{\partial \tau} - \frac{C^5}{R}\frac{\partial^2 F}{\partial y^2} - \frac{2-\gamma}{2\gamma C}\frac{\mathrm{d}C}{\mathrm{d}\tau}F = 0. \tag{44}$$

Here it is worth making a comment. When deriving equation (38) we, in particular, assumed that dissipation is weak. The condition $R \ll 1$ does not mean that dissipation is strong. Rather it means that dissipation dominates non-linearity. The condition that dissipation is weak means that the characteristic damping time of oscillations is much higher than the inverse oscillation frequency. We will discuss what restrictions must be imposed on the values of various quantities to satisfy this condition later.

We make the variable substitution

$$F = C^{\frac{2-\gamma}{2\gamma}}\widetilde{F}. \tag{45}$$

As a result equation (44) reduces to

$$\frac{\partial \widetilde{F}}{\partial \tau} = \frac{C^5}{R}\frac{\partial^2 \widetilde{F}}{\partial y^2}. \tag{46}$$

We look for the solution to this equation in the form $\widetilde{F}(y,\tau) = Y(y)\Theta(\tau)$. Substituting this expression in equation (46) and separating the variables yields

$$\frac{R}{C^5\Theta}\frac{\mathrm{d}\Theta(\tau)}{\mathrm{d}\tau} = \frac{1}{Y}\frac{\mathrm{d}^2 Y}{\mathrm{d}y^2} = \lambda, \tag{47}$$

where λ is a constant. Since $Y(y)$ must be a 2π-periodic function it follows that $\lambda = -n^2$, where $n = 1, 2, \ldots$ Below we only consider the fundamental harmonic and take $n = 1$. Then imposing the initial condition $F = -\sin y$ at $\tau = 0$ we obtain

$$Y = -\sin y, \quad \Theta = \exp\left(-\frac{1}{R}\int_0^\tau C^5(\tau')\,\mathrm{d}\tau'\right). \tag{48}$$

Using these expressions we obtain from equation (45)

$$F = -C^{\frac{2-\gamma}{2\gamma}}\exp\left(-\frac{1}{R}\int_0^\tau C^5(\tau')\,\mathrm{d}\tau'\right)\sin y. \tag{49}$$

Taking $C(\tau) = e^{-\alpha\tau}$ we reduce this expression to

$$F = -\exp\left(-\frac{1-e^{-5\alpha\tau}}{5\alpha R} - \frac{2-\gamma}{2\gamma}\alpha\tau\right)\sin y. \tag{50}$$

Since $\Phi(y) = -\sin y$ we obtain from equation (40) that $u/c_0 = 2\epsilon\sin(kx)$ at the initial time. Hence, the initial amplitude of the velocity is 2ϵ. Using equation (13) we obtain

$$X = \frac{1-e^{-\alpha\tau}}{\epsilon\alpha k}. \tag{51}$$

Then we obtain from equation (24)

$$\xi = \frac{1-e^{-\alpha\tau}}{\epsilon\alpha} - kx, \quad \eta = \frac{1-e^{-\alpha\tau}}{\epsilon\alpha} + kx. \tag{52}$$

Using equations (40) and (52) we obtain

$$u = 2\epsilon c_0\exp\left(-\frac{1-e^{-5\alpha\tau}}{5\alpha R} - \frac{2-\gamma}{2\gamma}\alpha\tau\right) \times \cos\frac{1-e^{-\alpha\tau}}{\epsilon\alpha}\sin(kx). \tag{53}$$

When $\alpha \to 0$, that is there is no heating or cooling, the damping time in the dimensionless variables is $\tau = 1$ and the oscillation frequency is ϵ^{-1}. Hence, in this case the damping time is much higher that the inverse oscillation frequency. When $|\alpha| \lesssim 1$ the damping time is close to unity. The instantaneous oscillation period $\Delta\tau$ at $\tau = \tau_0$ is defined by

$$\frac{1-e^{-\alpha(\tau_0+\Delta\tau)}}{\epsilon\alpha} - \frac{1-e^{-\alpha\tau_0}}{\epsilon\alpha} = 2\pi.$$

It follows from this equation that $\Delta\tau \approx 2\pi\epsilon e^{\alpha\tau_0}$ and the instantaneous wave frequency is $2\pi/\Delta\tau = \epsilon^{-1}e^{-\alpha\tau_0}$. We only consider $|\alpha|\tau_0 \le 1$, so the condition that the damping time is much higher than the inverse wave frequency is hold.

Summarizing, in the approximation $R \ll 1$ the evolution of the initial sinusoidal perturbation is simple: The spatial dependence remains sinusoidal, the solution oscillates with the slowly decreasing frequency, and the oscillation amplitude exponentially decays.

We note that we do not apply the results obtained in this section to interpreting observations and do not compare them with the results obtained in the previous linear studies of wave damping. Our only aim is to present a qualitative description of the wave evolution in the linear approximation.

5 SOLUTION FOR $R \gg 1$

In this section we consider the case of very small dissipative coefficients implying that $R \gg 1$. In this case we can neglect the third term in equation (38). Then this equation reduces to

$$\frac{\partial F}{\partial \tau} - \frac{\gamma+1}{2}F\frac{\partial F}{\partial y} - \frac{2-\gamma}{2\gamma C}\frac{\mathrm{d}C}{\mathrm{d}\tau}F = 0. \tag{54}$$

The equation of characteristics of this equation is

$$\frac{\mathrm{d}y}{\mathrm{d}\tau} = -\frac{\gamma+1}{2}F. \tag{55}$$

Let $y = y(\tau)$ be the equation of a characteristic. On this characteristic $F = F(\tau, y(\tau))$. Then the variation of F along this characteristic is described by

$$\frac{\mathrm{d}F}{\mathrm{d}\tau} = \frac{2-\gamma}{2\gamma c}\frac{\mathrm{d}c}{\mathrm{d}\tau}F. \tag{56}$$

The solution to this equation is

$$F = F_0 C^{\frac{2-\gamma}{2\gamma}}, \tag{57}$$

where F_0 is the value of F at $\tau = 0$. It follows from equation (43) that $F_0 = \Phi(y_0)$. Using this result and equation (57) we obtain from equation (55) that the equation of a characteristic is

$$y(\tau) = y_0 - \frac{\gamma+1}{2}\Phi(y_0)\int_0^\tau \left[C(\tau')\right]^{\frac{2-\gamma}{2\gamma}}\mathrm{d}\tau'. \tag{58}$$

To obtain the solution to equation (54) we need to express y_0 in terms of τ and y using equation (58) and substitute $y_0(\tau, y)$ in equation (57) with $F_0 = \Phi(y_0)$.

We consider an example taking $\Phi(y) = -\sin y$ and $T(t) = T_0 e^{-2\alpha\tau}$, where α is a constant; $\alpha < 0$ corresponds to heating and $\alpha > 0$ to cooling of a coronal loop. Then it follows that $C(\tau) = e^{-\alpha\tau}$ and equations (57) and (58) reduces to

$$F = -\sin y_0\, \mathrm{e}^{-\frac{2-\gamma}{2\gamma}\alpha\tau}, \tag{59}$$

$$y = y_0 + \frac{\gamma(\gamma+1)\sin y_0}{\alpha(2-\gamma)}\left(1 - e^{-\frac{2-\gamma}{2\gamma}\alpha\tau}\right) \equiv \Psi(\tau, y_0). \tag{60}$$

To obtain F as a function of τ and y we need to solve equation (60) with respect to y_0 thus expressing y_0 in terms of τ and y, and then substitute the result in equation (59). It is only possible to obtain y_0

as a single-valued function of τ and y when $\Psi(\tau, y_0)$ is a monotonic function of y_0. We obtain

$$\frac{\partial \Psi}{\partial y_0} = 1 + \frac{\gamma(\gamma+1)\cos y_0}{\alpha(2-\gamma)}\left(1 - e^{-\frac{2-\gamma}{2\gamma}\alpha\tau}\right). \quad (61)$$

Since $\partial\Psi/\partial y_0 > 0$ at $\tau = 0$ the condition that $\Psi(\tau, y_0)$ is a monotonic function of y_0 is

$$\frac{\gamma(\gamma+1)}{\alpha(2-\gamma)}\left(1 - e^{-\frac{2-\gamma}{2\gamma}\alpha\tau}\right) < 1. \quad (62)$$

When

$$\alpha > \alpha_c = \frac{\gamma(\gamma-1)}{2-\gamma} \quad (63)$$

the condition given by equation (62) is satisfied for any value of τ and consequently the solution to equation (54) exists for any τ. We obtain $\alpha_c = 40/3$ for $\gamma = 5/3$. When $\alpha < \alpha_c$ the condition given by equation (62) is only satisfied when

$$\tau < \tau_c = -\frac{2\gamma}{\alpha(2-\gamma)}\ln\left(1 - \frac{\alpha(2-\gamma)}{\gamma(\gamma+1)}\right). \quad (64)$$

It is proved in Paper I that τ_c is a monotonically increasing function of α. When $\alpha \to \alpha_c$ we obtain $\tau_c \to \infty$.

It follows from equation (60) that

$$\frac{\partial y_0}{\partial y} = \left(\frac{\partial \Psi}{\partial y_0}\right)^{-1}. \quad (65)$$

Differentiating equation (57) with $F_0 = \Phi(y_0)$ yields

$$\frac{\partial F}{\partial y} = \frac{\partial \Phi}{\partial y_0}\left(\frac{\partial \Psi}{\partial y_0}\right)^{-1} C^{\frac{2-\gamma}{2\gamma}}. \quad (66)$$

When τ is fixed $\partial\Psi/\partial y_0$ takes minimum at $y_0 = \pi$. Then $\partial\Psi/\partial y_0 \to 0$ as $\tau \to \tau_c$ at $y_0 = \pi$. Since in accordance with equation (60) $y = \pi$ when $y_0 = \pi$ it follows from equation (66) that

$$\left.\frac{\partial F}{\partial y}\right|_{y=\pi} \to \infty \quad \text{as} \quad \tau \to \tau_c. \quad (67)$$

This phenomenon is called a gradient catastrophe that is previously studied, for example, in non-linear acoustics (e.g. Rudenko & Soluyan 2001), hydrodynamics (e.g. Landau & Lifshitz 1987; Ruderman 2019), and in the general theory of waves (e.g. Whitham 1974). We now discuss what happens with u given by equation (40). It follows from this equation that

$$\frac{\partial u}{\partial x} = -\epsilon k c_0\left(\frac{\partial F}{\partial \xi} + \frac{\partial F}{\partial \eta}\right). \quad (68)$$

Then we obtain from equations (67) and (68) that

$$\left.\frac{\partial u}{\partial x}\right|_{x=x_c} \to -\infty \quad \text{as} \quad \tau \to \tau_c \quad (69)$$

if x_c satisfies one of the two equations,

$$\begin{aligned} &kX(\tau_c) - kx_c = \pi \pmod{2\pi}, \\ &kX(\tau_c) + kx_c = \pi \pmod{2\pi}, \end{aligned} \quad (70)$$

and the restriction $kx_c \in [0, \pi]$, where $X(\tau)$ is defined by equation (51). If both equations in (70) are satisfied then we obtain $2kx_c = 0 \pmod{2\pi}$, which implies that either $x_c = 0$ or $kx_c = \pi$.

There is $\chi \in [0, 2\pi)$ and a positive integer n such that $kX(\tau_c) = 2\pi n + \chi$. Let us assume that there is no x_c satisfying the first equation in (70). Since kx_c can vary from 0 to π this is only possible when $\chi < \pi$. However, in this case we can find x_c satisfying the second equation in (70). Hence, there is always x_c such that $kx_c \in [0, \pi]$ and u has an infinite derivative with respect to x at $x = x_c$ and $\tau = \tau_c$. A shock starts to form at $x = x_c$ and $\tau = \tau_c$.

We introduce the dimensionless velocity $U = u(2\epsilon c_0)^{-1}$. This quantity can be expanded in the Fourier series

$$U = \sum_{n=1}^{\infty} A_n(\tau)\sin(nkx), \quad (71)$$

$$A_n(\tau) = \frac{2}{L}\int_0^L U(x,\tau)\sin(nkx)\,dx. \quad (72)$$

It is shown in Appendix B that the expression for $A_n(\tau)$ is given by

$$\begin{aligned} A_n(\tau) = (-1)^{n+1} e^{-\frac{2-\gamma}{2\gamma}\alpha\tau}\cos(nkX)\Big\{ J_{n-1}(ns(\tau)) \\ - J_{n+1}(ns(\tau)) - \frac{s(\tau)}{2}[J_{n-2}(ns(\tau)) - J_{n+2}(ns(\tau))]\Big\}, \end{aligned} \quad (73)$$

where

$$s(\tau) = \frac{\gamma(\gamma+1)}{\alpha(2-\gamma)}\left(1 - e^{-\frac{2-\gamma}{2\gamma}\alpha\tau}\right). \quad (74)$$

The dependence of U on τ for various values of α is shown in Fig. 1 for $\epsilon = 0.094/|\alpha|$ when $\alpha \neq 0$, and $\epsilon = 0.094$ when $\alpha = 0$. The reason for choosing these values of ϵ are explained below. In this figure the evolution of the perturbation is shown up to the instance of gradient catastrophe for the cases when the temperature increases ($\alpha = -1$), the temperature does not change ($\alpha = 0$), and the temperature decreases ($\alpha = 1$). Since $\alpha_c < 14$ the lower right panel in Fig. 1 corresponds to the case where the gradient catastrophe does not occur. Since $\tau_c \approx 0.73$ for $\alpha = -1$ and $\tau_c \approx 0.78$ for $\alpha = 1$ the loop temperature increases approximately four times in the first case and decreases approximately five times in the second case when τ varies from 0 to τ_c. In accordance with this estimate we chose to show the evolution of U for τ varying from 0 to 0.057 because the loop temperature decreases approximately five times for $\alpha = 14$ and $\tau = 0.057$.

We also show the dependences of A_n on τ for $n = 1, 2, 3$ in Fig. 2. An important property of the evolution of initial oscillation is that sometimes the perturbation looks not as a fundamental mode but as the first overtone. It is especially clear in the upper right panel in the perturbation shown by the solid line. This property is also confirmed in Fig. 2 where there are some values of τ such that $A_1(\tau) \approx 0$, while $|A_2(\tau)|$ take a local maximum. This phenomenon only occurs when the initial perturbation amplitude is relatively large, that is for $\alpha = 0$ and $\alpha = \pm 1$. As for the case with small amplitude corresponding to $\alpha = 14$, the amplitude of the fundamental harmonic is much higher than those of the overtones. Hence, it is obvious that the phenomenon described above is caused by non-linearity.

Now we discuss the results obtained in this section using the dimensional variables. The temperature in a cooling coronal loop is given by

$$T_0(t) = T_{00}e^{-t/t_{\rm cool}}, \qquad t_{\rm cool} = \frac{L}{2\pi\epsilon|\alpha|c_0}. \quad (75)$$

We take $T_{00} = 6$ MK. This yields $c_0 \approx 370$ km s^{-1}. Then taking $L = 218$ Mm $= 2.18 \times 10^8$m we obtain

$$t_{\rm cool} \approx \frac{94}{\epsilon|\alpha|}\ \text{s}. \quad (76)$$

Now we discuss when the approximation $R \gg 1$ can be used. We take $n_0 = 10^{15}$ m^{-3} as a typical value of the electron concentration in coronal loops. It is shown in Paper I that $\nu_0 \approx 8 \times 10^{11}$ m^{2}s^{-1} and $\kappa_0 \approx 2.55 \times 10^{13}$ m^{2}s^{-1} for this value of n_0 and $T_{00} = 6$ MK. Then taking $\gamma = 5/3$ we obtain from equation (39)

$$R \approx 4.67\epsilon. \quad (77)$$

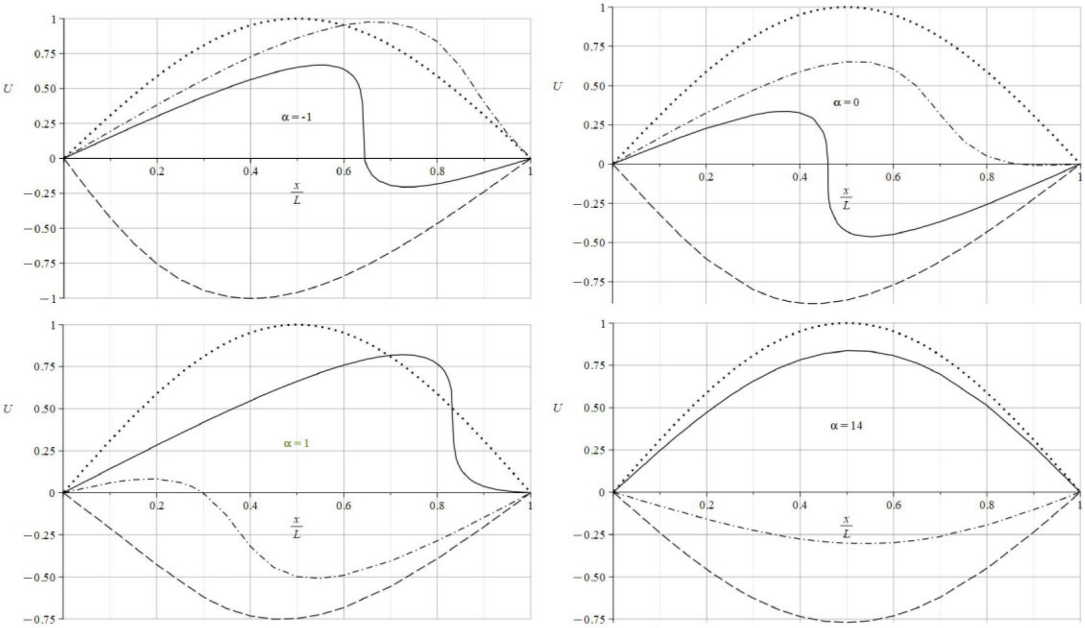

Figure 1. Dependence of U on x/L for $R \gg 1$ and various values of α. In the upper panels and left lower panel the dotted, dashed, dash-dotted, and solid lines correspond to $\tau = 0$, $\tau_c/3$, $2\tau_c/3$, and τ_c. In the lower right panel the dotted, dashed, dash-dotted, and solid lines correspond to $\tau = 0$, 0.019, 0.038, and 0.057.

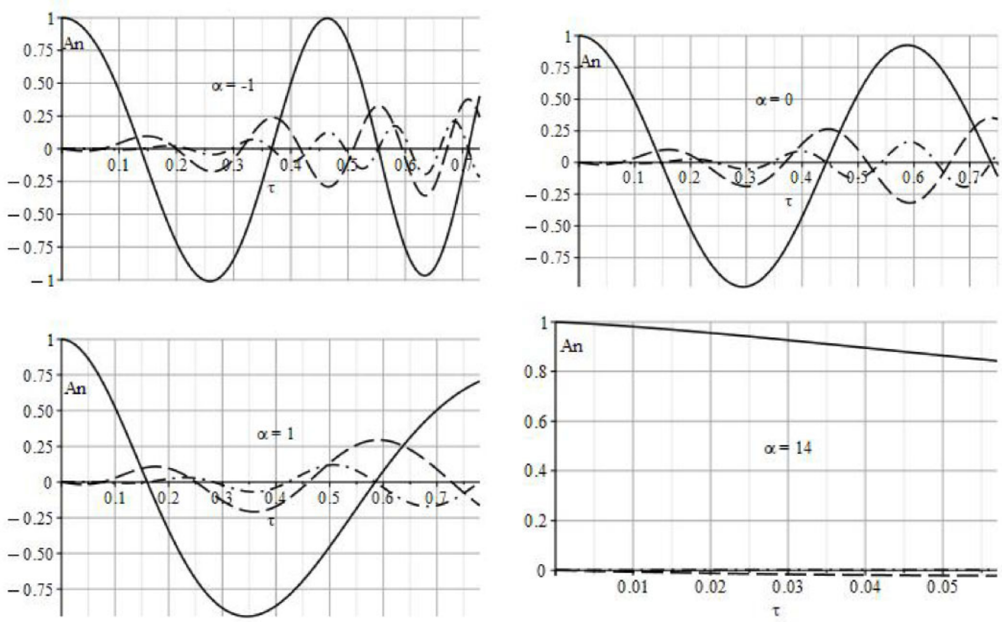

Figure 2. Dependence of Fourier coefficients A_n in equation (71) on τ for $R \gg 1$ and various values of α. The solid, dashed, and dash-dotted lines correspond to $n = 1$, 2, and 3, respectively.

Since by assumption ϵ is substantially less than 1 it follows that for chosen values of L, T_{00}, and n_0 the condition $R \gg 1$ cannot be satisfied. Hence, we considered this limiting case just for completeness. We can obtain $R \gg 1$ by increasing n_0 by two orders of magnitude since it is quite possible to have $n_0 = 10^{17}\,\mathrm{m}^{-3}$ in flaring coronal loops. In that case

$$R \approx 467\epsilon, \tag{78}$$

and we obtain $R \gtrsim 40$ for $\epsilon \gtrsim 0.1$.

It follows from equation (76) that for given α we can either choose ϵ and calculate t_{cool}, or choose t_{cool} and calculate ϵ. We made the second option and took $t_{\mathrm{cool}} = 1000$ s. Then we obtained $\epsilon = 0.094$ for $|\alpha| = 1$ and $\epsilon = 0.0067$ for $|\alpha| = 14$. Since the initial amplitude of perturbation is $2\epsilon c_0$, the relative amplitude of the initial perturbation, u_0/c_s, is 0.188 in the first case and 0.0134 in the second case.

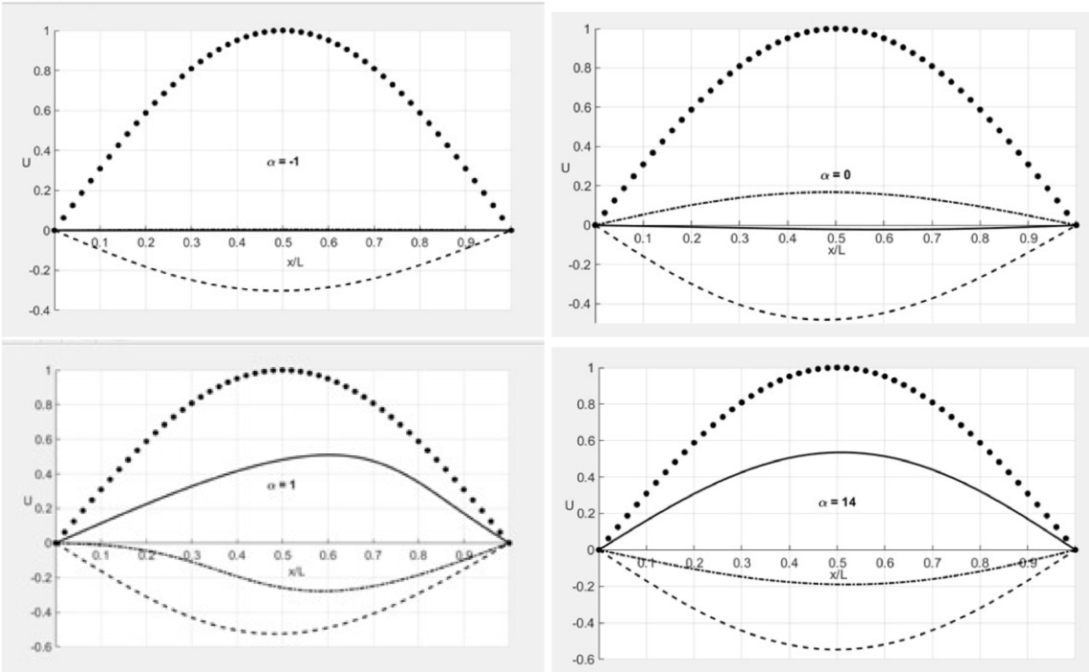

Figure 3. Dependence of U on x/L for various values of α and τ, and R given by equation (77). In the upper and left lower panels the dotted, dashed, dash-dotted, and solid lines correspond to $\tau = 0,\ \tau_c/3,\ 2\tau_c/3$, and τ_c. In the right lower panel the dotted, dashed, dash-dotted, and solid lines correspond to $\tau = 0,\ 0.019,\ 0.038$, and 0.057.

6 GENERIC CASE

In this section we consider the generic case and study the simultaneous effect of non-linearity and dissipation. To do this we solve equation (38) and then use the expression of U in terms of F. The results of this calculation are presented in Fig. 3 where the dependence of U on x/L is shown for four different values of τ. We use the same parameters as in the previous section. In particular, we take $\epsilon = 0.094$ for $\alpha = -1$, 0, and 1, and $\epsilon = 0.0067$ for $|\alpha| = 14$. Then it follows from equation (77) that $R \approx 0.44$ for $\alpha = -1$, 0, and 1, and $R \approx 0.031$ for $|\alpha| = 14$. We do not see any effect of non-linearity in the upper panels and the right lower panel in Fig. 3. It is not surprising because $R < 0.5$ and consequently dissipation dominates non-linearity. We also see in the left upper panel in Fig. 3 that the two curves in this panel corresponding to higher values of τ coincide with the horizontal axis. This implies that at these value of τ the perturbation is close to zero. This effect is due to exponential increase of dissipative coefficients for $\alpha = -1$.

The effect of non-linearity is only manifested in the left lower panel in Fig. 3 corresponding to $\alpha = 1$. For this value of α the dissipation coefficients exponentially decrease so the coefficient at the last but one term in equation (38) becomes more than 30 times less than its initial value at the end of perturbation evolution corresponding to the solid curve in Fig. 3. However the evolution of perturbation shown in the left lower panel in Fig. 3 is still very much different from that shown in the left lower panel in Fig. 1 obtained for $R \gg 1$. The strong reduction in the coefficient at the last but one term in equation (38) for the values of τ corresponding to the perturbation amplitude strongly reduced in comparison with its initial value. As a result for these values of τ the effect of dissipation is comparable with that of non-linearity however it does not dominate. In Fig. 4 the continuous evolution of U is shown. The results shown in this figure confirm the conclusion about the properties of the perturbation evolution made using Fig. 3.

We also studied standing slow waves in a coronal loop with the same parameters as before however with the plasma density increased by two orders of magnitude. As was explained in the previous section in this case R also increases by two orders of magnitude and it is given by equation (78). As a result we obtain $R \approx 44$ for $\alpha = -1$, 0, and 1, and $R \approx 3.1$ for $|\alpha| = 14$. The results of this calculation are presented in Fig. 5. We compare the curves shown in this figure with those shown in Fig. 1. We start from the left upper panels. In Fig. 5 the effect of non-linearity is pronounced, but does not dominate. The reason is that although the coefficient at the last but one term in equation (38) is initially small ($R = 40$), it exponentially increases with time and becomes of the order of unity for $\tau \gtrsim 2\tau_c/3$. As a result, the solid curve in the left upper panel in Fig. 5 is very much different from that in the left upper panel in Fig. 1. On the other hand, the right panel in Fig. 5 is very similar to that in Fig. 1. Finally, the curves in the lower panel in Fig. 5 practically coincide with the corresponding curves in the lower panel in Fig. 1. It is an expected result because not only the coefficient at the last but one term in equation (38) is small at $\tau = 0$, but it also exponentially decreases with time. In Fig. 6 the continuous evolution of U is shown. The results shown in this figure confirm the conclusion about the properties of the perturbation evolution made using Fig. 5.

An important conclusion that follows from the inspection of Figs 4 and 6 is that cooling decelerates the wave damping. It is an expected result because plasma cooling causes an exponential reduction of the dissipative coefficients.

7 SUMMARY AND CONCLUSIONS

We studied non-linear standing sausage waves in a coronal magnetic loop with a variable temperature. We used the simplest model of a coronal loop which is a straight magnetic tube with a circular

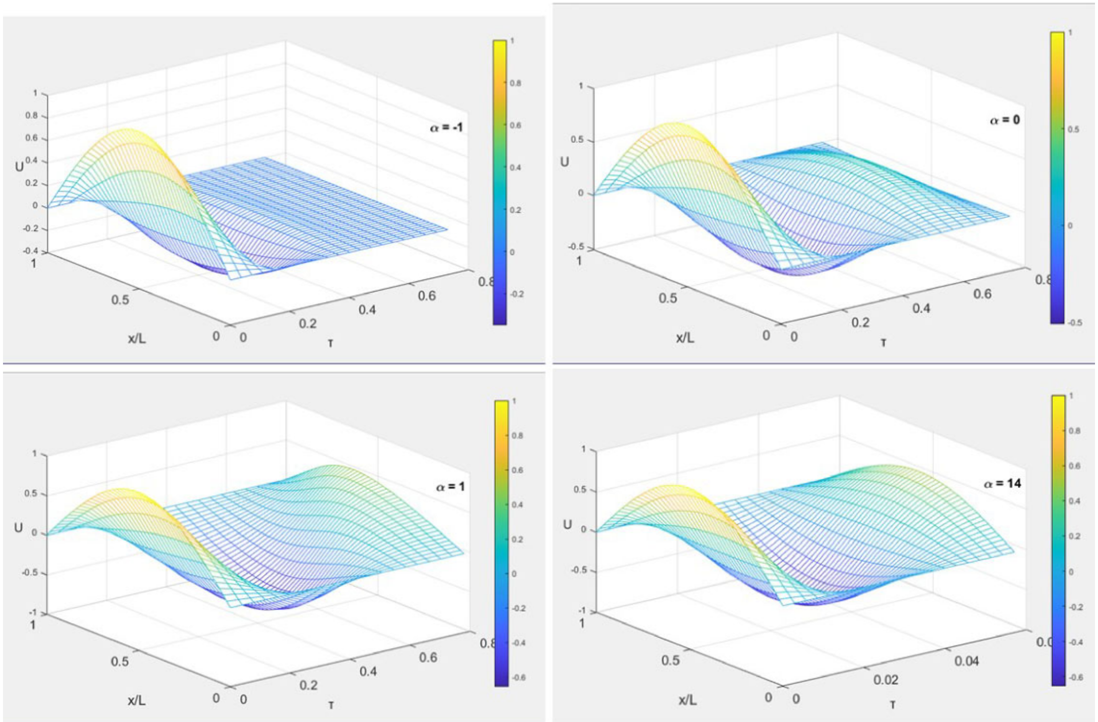

Figure 4. Continuous evolution of the dependence of U on x/L for various values of α and R given by equation (77).

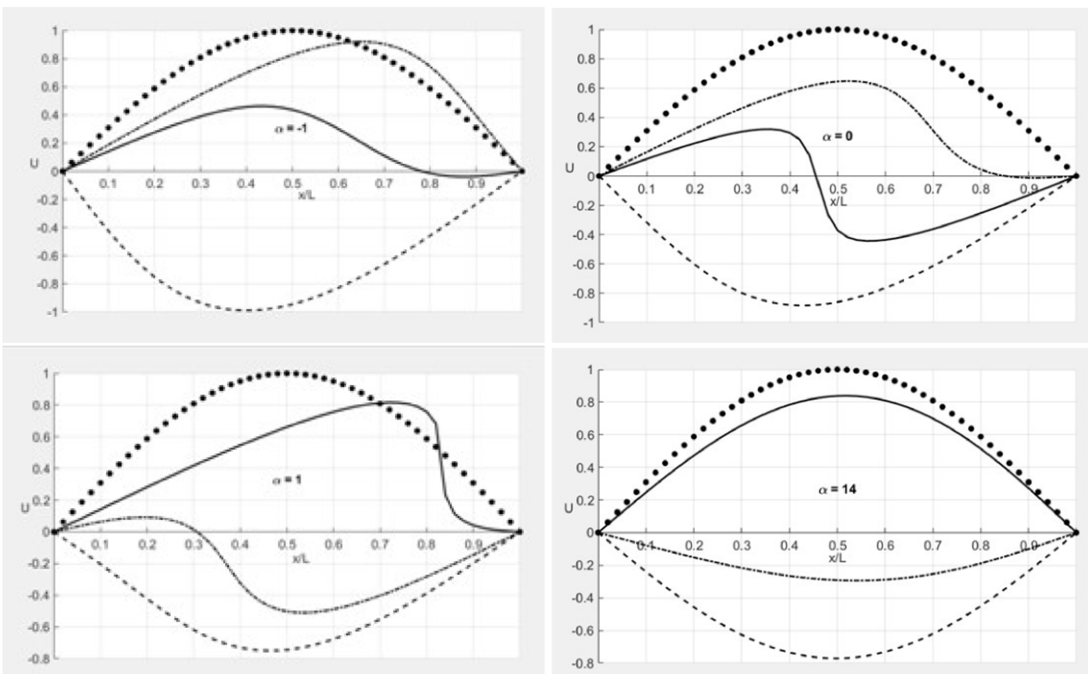

Figure 5. Dependence of U on x/L for various values of α and τ, and R given by equation (78). In the upper and left lower panels the dotted, dashed, dash-dotted, and solid lines correspond to $\tau = 0,\ \tau_c/3,\ 2\tau_c/3$, and τ_c. In the right lower panel the dotted, dashed, dash-dotted, and solid lines correspond to $\tau = 0,\ 0.019,\ 0.038$, and 0.057.

cross-section of constant radius and constant plasma densities inside and outside the tube. We assumed that the plasma-beta is low. This enables us to neglect the magnetic field perturbation and consider the sausage oscillations as occurring in a tube with a rigid boundary. Then these oscillations are described by pure 1D gas-dynamic equations. It is assumed that while the temperature of plasma in the tube can vary, its density remains constant.

We also assumed that the perturbation amplitude is small and used the reductive perturbation method to derive the governing equations for non-linear standing sausage waves. We showed that

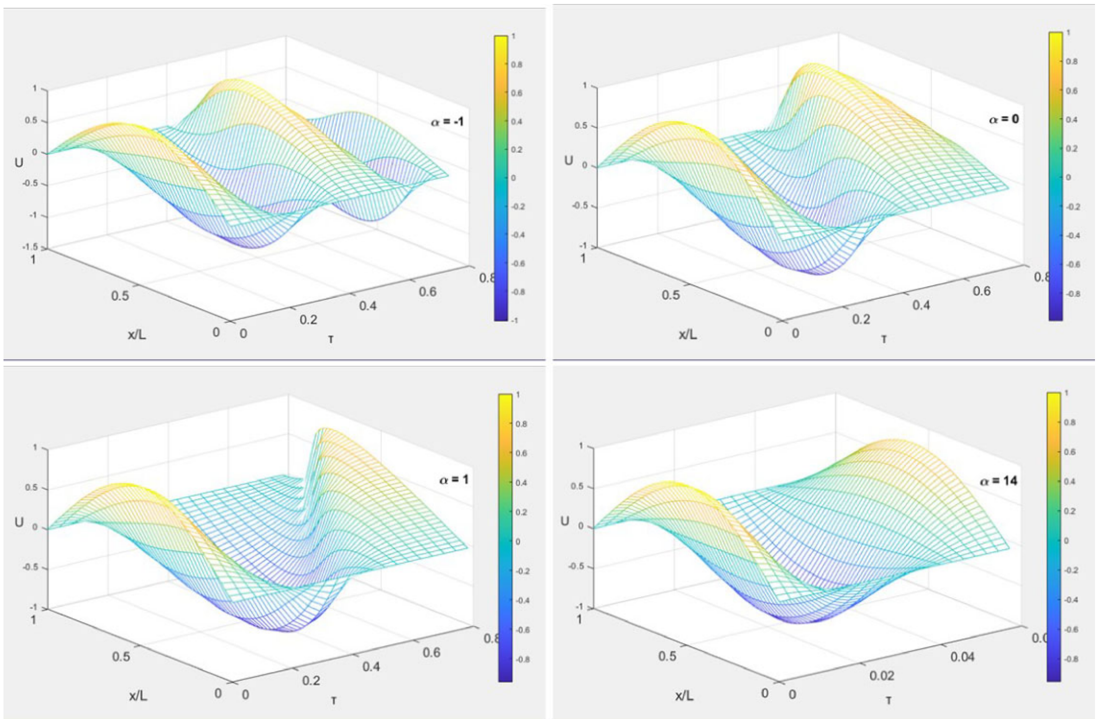

Figure 6. Continuous evolution of the dependence of U on x/L for various values of α and R given by equation (78).

the solution describing a standing non-linear wave is the sum of two identical non-linear waves propagating in the opposite directions similar to a standing linear wave. Each of the two propagating waves is described by a modified Burgers equation that reduces to the classical Burgers equation (Burgers 1948) when the temperature of plasma inside the magnetic tube does not change.

After that we considered three different cases. In the first case we assumed that dissipation strongly dominates non-linearity. In this case each of the two waves propagating in the opposite directions is described by the linearized modified Burgers equation. Then the solution to the problem is straightforward. In particular the solution describing the fundamental harmonic is a sin function of the spatial variable times a function describing the variation of the wave amplitude due to dissipation and variation of the plasma temperature inside the tube. This solution is given by equation (53).

In the second case we assumed that non-linearity strongly dominates dissipation so the latter can be neglected. In this case the ideal counterpart of the modified Burgers equation was solved using the method of characteristics. An important property is that in general the evolution of an initial perturbation results in a gradient catastrophe where an infinite gradient appears in the perturbation profile. However, strong cooling can prevent the gradient catastrophe.

In the third case we studied the competition between non-linearity and dissipation. In this case the modified Burges equation describing the two counterpropagating non-linear waves was solved numerically. We considered two cases: A relatively rarified coronal loop with the plasma density equal to $10^{15}\,\mathrm{kg\,m^{-3}}$, and a dense loop with the plasma density equal to $10^{17}\,\mathrm{kg\,m^{-3}}$. In the case of rarified loop dissipation dominates and the effect of non-linearity is only weakly pronounced. In contrast, in the case of dense loop non-linearity dominates and the evolution of the initial perturbation is very similar to that in the case without dissipation. The only difference is that the gradient catastrophe does not occur being prevented by dissipation. The most important conclusion that follows from our results is that the plasma cooling decelerates the wave damping. This is an expected effect because cooling results in the decrease of coefficients of viscosity and thermal conduction. This leads to weakening of dissipation.

DATA AVAILABILITY

There are no new data associated with this article.

REFERENCES

Abramowitz M., Stegun I. A., 2004, Handbook of Mathematical Functions. Dover, New York

Al-Ghafri K. S., 2015, J. Astrophys. Astron., 36, 325

Al-Ghafri K. S., Ruderman M. S., Williamson A., Erdélyi R., 2014, ApJ, 786, 36

Aschwanden M. J., Terradas J., 2008, ApJ, 686, L127

Burgers J. M., 1948, in von Mises R., von Karman T., eds, Advances in Applied Mechanics. Academic Press Inc, New York, p. 171

Braginskii S. I., 1965, in Leontovich M. A., ed., Transport processes in plasma. Reviews of Plasma Physics. Vol. 1, Consultants Bureau, New York, p. 205

De Moortel I., Hood A. W., 2003, A&A, 408, 755

De Moortel I., Hood A. W., 2004, A&A, 415, 705

Goedbloed J. P. H., Poedts S., 2004, Principles of Magnetohydrodynamics. Cambridge Univ. Press, Cambridge, UK

Kakutani T., Ono H., Taniuti T., Wei C.-C., 1968, J. Phys. Soc. Japen, 24, 1159

Kliem B., Dammasch I. E., Curdt W., Wilhelm K., 2002, ApJ, 568, L61

Kolotkov D. Y., Nakariakov V. M., 2022, MNRAS, 514, L51

Kolotkov D. Y., Duckenfield T. J., Nakariakov V. M., 2020, A&A, 644, A33

Kolotkov D. Y., Zavershinskii D., Nakariakov V. M., 2021, Plasma Phys. Control. Fusion, 63, 124008

Korn G. A., Korn T. M., 1961, Mathematical Handbook for Scientists and Engineers. Dover Publications, Inc, Mineola, NY, USA

Landau L. D., Lifshitz E. M., 1987, Fluid Mechanics, Course of Theoretical Physics. Vol. 6, Pergamon Press, Oxford, UK
Mendoza-Briceño C. A., Erdélyi R., Sigalotti L. D. G., 2004, ApJ, 568, L61
Morton M. J., Erdélyi R., 2009, ApJ, 707, 750
Morton M. J., Erdélyi R., 2010, A&A, 519, A43
Nakariakov V. M., Zhong S. H., Kolotkov D. Y, Meadowcroft R. L., Zhong Y., Yuan D., 2024, Rev. Modern Plasma Phys., 8, 19
Ofman L., Wang T., 2002, ApJ, 580, L85
Pandey V. S., Dwivedi B. N., 2006, Solar Phys., 236, 127
Priest E., 1982, Solar Mangneto-Hydrodynamics. Kluver Academic Publishers, Dordrecht
Rudenko O. V., Soluyan S. I., 2001, Theoretical Foundation of Nonlinear Acoustics. Consultant Bureau, New York
Ruderman M. S., 2011a, Solar Phys., 271, 41
Ruderman M. S., 2011b, A&A, 534, A78
Ruderman M. S., 2013, A&A, 553, A23
Ruderman M. S., 2019, Fluid Dynamics and Linear Elasticity. Springer, Switzerland
Ruderman M. S., Petrukhin N. S., Kataeva L. Y., 2025, Solar Phys., 300, 85
Sigalotti L. D. G., Mendoza-Briceño C. A., Luna-Cardozo M., 2007, Solar Phys., 247, 187
Spitzer L. J., 1962, Physics of Fully Ionazed Gases. Wiley Interscience, New York
Taniuti T., Wei C.-C., 1968, J. Phys. Soc. Japen, 24, 941
Verwichte E., Haynes M., Arber T. D., Brady C. S., 2008, ApJ, 685, 1286
Wang T., 2011, Space Sci. Rev., 158, 397
Wang T., Solanki S. K., Curdt W., Innes D. E., Dammasch I. E., 2002, ApJ, 574, L101
Wang T., Solanki S. K., Innes D. E., Curdt W., Marsch E., 2003a, A&A, 402, L17
Wang T., Solanki S. K., Curdt W., Innes D. E., Dammasch I. E., Kliem B., 2003b, A&A, 406, 1105
Wang T., Ofman L., Yuan D., Reale F., Kolotkov D. Y., Srivastava A. K., 2021, Space Sci. Rev., 217, 34
Whitham G. B., 1974, Linear and Non-Linear Waves. John Willey and Sons, New York

APPENDIX A: DERIVATION OF EXPRESSION FOR THE FOURIER TRANSFORM OF THE RIGHT-HAND SIDE OF EQUATION (32)

Since $f(y,t_1)$ is a periodic function of y with the period 2π it can be expanded in the Fourier series

$$f(y,t_1) = \sum_{n=-\infty}^{\infty} f_n(t_1)e^{iny}, \tag{A1}$$

where $f_0(t_1)=0$ and $f_{-n}(t_1)=f_n^*(t_1)$ with the asterisk indicating complex conjugate. Using the identity (Korn & Korn 1961)

$$\sum_{n=-\infty}^{\infty} a_n \sum_{m=-\infty}^{\infty} b_m = \sum_{n=-\infty}^{\infty}\sum_{m=-\infty}^{\infty} a_m b_{n-m}, \tag{A2}$$

we obtain

$$g(y)h(y) = \sum_{n=-\infty}^{\infty} e^{iny} \sum_{m=-\infty}^{\infty} g_m h_{n-m}, \tag{A3}$$

where $g(y)$ and $h(y)$ are 2π-periodic real functions.

Now we obtain the Fourier expansions for various terms on the right-hand side of equation (33). Using equation (A1) we obtain

$$f'_\pm = \sum_{n=-\infty}^{\infty} inf_n e^{ikn(X\pm x)}. \tag{A4}$$

Using this result yields

$$\begin{aligned} f'_- - f'_+ &= \sum_{n=-\infty}^{\infty} 2nf_n e^{iknX}\sin(nkx) \\ &= 2\sum_{n=1}^{\infty} n\left(f_n e^{iknX} + f_n^* e^{-iknX}\right)\sin(nkx), \end{aligned} \tag{A5}$$

$$f'''_- - f'''_+ = -2\sum_{n=1}^{\infty} n^3\left(f_n e^{iknX} + f_n^* e^{-iknX}\right)\sin(nkx). \tag{A6}$$

Next using equation (A3) yields

$$f'^2_\pm = -\sum_{n=-\infty}^{\infty} e^{ikn(X\pm x)} \sum_{m=-\infty}^{\infty} m(n-m) f_m f_{n-m}. \tag{A7}$$

With the aid of this result we obtain

$$\begin{aligned} f'^2_- - f'^2_+ &= 2i\sum_{n=-\infty}^{\infty} e^{iknX}\sin(nkx) \sum_{m=-\infty}^{\infty} m(n-m) f_m f_{n-m} \\ &= 2i\sum_{n=1}^{\infty}\sin(nkx)\sum_{m=-\infty}^{\infty} m(n-m)\big(f_m f_{n-m}e^{iknX} \\ &\quad - f_m^* f_{n-m}^* e^{-iknX}\big), \end{aligned} \tag{A8}$$

Again using equation (A3) we obtain

$$f_\pm f''_\pm = -\sum_{n=-\infty}^{\infty} e^{ikn(X\pm x)} \sum_{m=-\infty}^{\infty} m^2 f_m f_{n-m}. \tag{A9}$$

Using this result yields

$$\begin{aligned} f_- f''_- - f_+ f''_+ &= 2i\sum_{n=-\infty}^{\infty} e^{iknX}\sin(nkx)\sum_{m=-\infty}^{\infty} m^2 f_m f_{n-m} \\ &= 2i\sum_{n=1}^{\infty}\sin(nkx)\sum_{m=-\infty}^{\infty} m^2\big(f_m f_{n-m}e^{iknX} \\ &\quad - f_m^* f_{n-m}^* e^{-iknX}\big). \end{aligned} \tag{A10}$$

Using equation (A1) we obtain

$$\begin{aligned} f_- f''_+ &= -\sum_{m=-\infty}^{\infty} f_m e^{ikm(X-x)} \sum_{l=-\infty}^{\infty} l^2 f_l e^{ikl(X+x)} \\ &= -\sum_{m=-\infty}^{\infty}\sum_{l=-\infty}^{\infty} l^2 f_l f_m e^{ik(l-m)x} e^{ik(m+l)X}. \end{aligned} \tag{A11}$$

Making the variable substitution $l = n + m$ and then changing the order of summation we transform this expression to

$$f_- f''_+ = -\sum_{n=-\infty}^{\infty} e^{iknx} \sum_{m=-\infty}^{\infty} (m+2n)^2 f_m f_{n+m} e^{ikX(n+2m)}. \tag{A12}$$

To obtain the expression for $f_+ f''_-$ we only need to substitute $-x$ for x in this equation. Then we arrive at

$$\begin{aligned} f_- f''_+ - f_+ f''_- &= -2i\sum_{n=-\infty}^{\infty}\sin(knx) \\ &\quad\times \sum_{m=-\infty}^{\infty} (m+2n)^2 f_m f_{n+m} e^{ikX(n+2m)}. \end{aligned} \tag{A13}$$

Finally we transform this expression to

$$\begin{aligned} f_- f''_+ - f_+ f''_- &= -2i\sum_{n=1}^{\infty}\sin(knx)\sum_{m=-\infty}^{\infty}(m+2n)^2 \\ &\quad\times\left(f_m f_{n+m} e^{ikX(n+2m)} - f_m^* f_{n+m}^* e^{-ikX(n+2m)}\right). \end{aligned} \tag{A14}$$

APPENDIX B: CALCULATION OF FOURIER COEFFICIENTS

Using equation (40) we obtain from equation (72)

$$A_n(\tau) = \frac{1}{L}\int_0^L [F(\xi) - F(\eta)]\sin(nkx)\,\mathrm{d}x. \tag{B1}$$

Using the variable substitution we transform this expression to

$$\begin{aligned} A_n(\tau) = &-\frac{1}{\pi}\int_{kX}^{kX-\pi} F(\xi)\sin[n(kX-\xi)]\,\mathrm{d}\xi \\ &-\frac{1}{\pi}\int_{kX}^{kX+\pi} F(\xi)\sin[n(\eta-kX)]\,\mathrm{d}\eta \\ &-\frac{1}{\pi}\int_{kX-\pi}^{kX+\pi} F(y)\sin[n(y-kX)]\,\mathrm{d}y \\ &= \frac{1}{\pi}\int_{\pi}^{\pi} F(y)[\cos(ny)\sin(nkX) - \sin(ny)\cos(nkX)]\,\mathrm{d}y. \end{aligned} \tag{B2}$$

When deriving this expression we used the fact that $F(y)$ is a 2π-periodic function. Now we make the variable substitution $y = y(y_0)$, where the function $y(y_0)$ is given by equation (60). Then using equation (59) we transform the expression for $A_n(\tau)$ to

$$\begin{aligned} A_n(\tau) = &\frac{1}{\pi}e^{-\frac{2-\gamma}{2\gamma}\alpha\tau}\int_{-\pi}^{\pi}\{\cos(nkX)]\sin[n(y_0 + s(\tau)\sin y_0)] \\ &- \sin(nkX)\cos[n(y_0 + s(\tau)\sin y_0)]\} \\ &\times [1 + s(\tau)\cos y_0)]\sin y_0\,\mathrm{d}y_0, \end{aligned} \tag{B3}$$

where

$$s(\tau) = \frac{\gamma(\gamma+1)}{\alpha(2-\gamma)}\left(1 - e^{-\frac{2-\gamma}{2\gamma}\alpha\tau}\right). \tag{B4}$$

The product of the second term in the curly brackets with the other terms in equation (B3) is odd with respect to y_0. This implies that the integral of this product is zero. The product of the first term in the curly brackets with the other terms in equation (B3) is even with respect to y_0. This implies that the integral of this product can be reduced to the integral over the interval $[0, \pi]$. Hence the expression for $A_n(\tau)$ can be reduced to

$$\begin{aligned} A_n(\tau) = &\frac{2}{\pi}e^{-\frac{2-\gamma}{2\gamma}\alpha\tau}\cos(nkX) \\ &\times\int_0^{\pi}\sin[n(y + s(\tau)\sin y)][1 + s(\tau)\cos y)]\sin y\,\mathrm{d}y, \end{aligned} \tag{B5}$$

where we dropped the subscript 0 at y. Using the relation (Abramowitz & Stegun 1964)

$$J_n(z) = \int_0^{\pi}\cos(z\sin\theta - n\theta)\,\mathrm{d}\theta, \tag{B6}$$

where $J_n(z)$ is the Bessel function, we obtain

$$\begin{aligned} &\frac{2}{\pi}\int_0^{\pi}\sin[n(y + s(\tau)\sin y)][1 + s(\tau)\cos y)]\sin y\,\mathrm{d}y \\ &= \frac{1}{\pi}\int_0^{\pi} F(\xi)\cos[(n-1)y + ns(\tau)\sin y]\,\mathrm{d}y \\ &-\frac{1}{\pi}\int_0^{\pi} F(\xi)\cos[(n+1)y + ns(\tau)\sin y]\,\mathrm{d}y \\ &+\frac{s(\tau)}{2\pi}\int_0^{\pi} F(\xi)\cos[(n-1)y + ns(\tau)\sin y]\,\mathrm{d}y \\ &-\frac{s(\tau)}{2\pi}\int_0^{\pi} F(\xi)\cos[(n+1)y + ns(\tau)\sin y]\,\mathrm{d}y \\ &= (-1)^{n+1}\Big\{J_{n-1}(ns(\tau)) - J_{n+1}(ns(\tau)) \\ &-\frac{s(\tau)}{2}[J_{n-2}(ns(\tau)) - J_{n+2}(ns(\tau))]\Big\}. \end{aligned} \tag{B7}$$

When deriving this expression we used the relation $j_{-n}(-z) = (-1)^n J_n(z)$. Substituting equation (B7) in equation (B5) we arrive at equation (73).

This paper has been typeset from a TEX/LATEX file prepared by the author.